

## Supporting Information

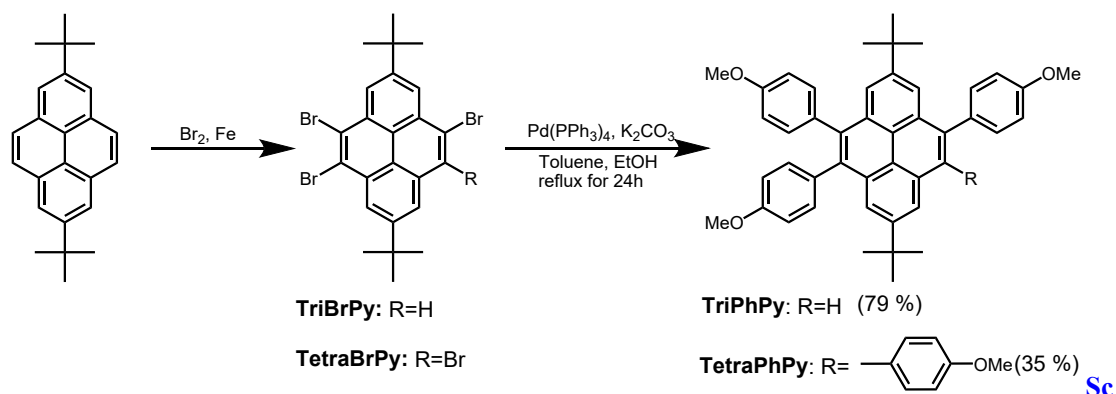
### Substituent dependent deep-blue pyrene-based chemosensor for trace nitroanilines sensing

Hua-Long Li,<sup>‡a</sup> Jing-Yi Cao,<sup>‡a</sup> Ze-Dong Yu,<sup>a</sup> Guang Yang,<sup>a</sup> Zeng-Min Xue,<sup>a</sup> Chuan-Zeng Wang<sup>\*a,b</sup> Wen-Xuan Zhao,<sup>a</sup> Yi Zhao,<sup>\*a</sup> Carl Redshaw,<sup>c</sup> and Takehiko Yamato,<sup>\*b</sup>

<sup>a</sup> School of Chemistry and Chemical Engineering, Shandong University of Technology, Zibo 255049, P. R. China

<sup>b</sup> Department of Applied Chemistry, Faculty of Science and Engineering, Saga University Honjo-machi 1, Saga 840-8502 Japan

<sup>c</sup> Chemistry, School of Natural Sciences, The University of Hull, Cottingham Road, Hull, Yorkshire HU6 7RX, UK



**heme S1.** Synthetic procedure for the substituted pyrene derivatives.

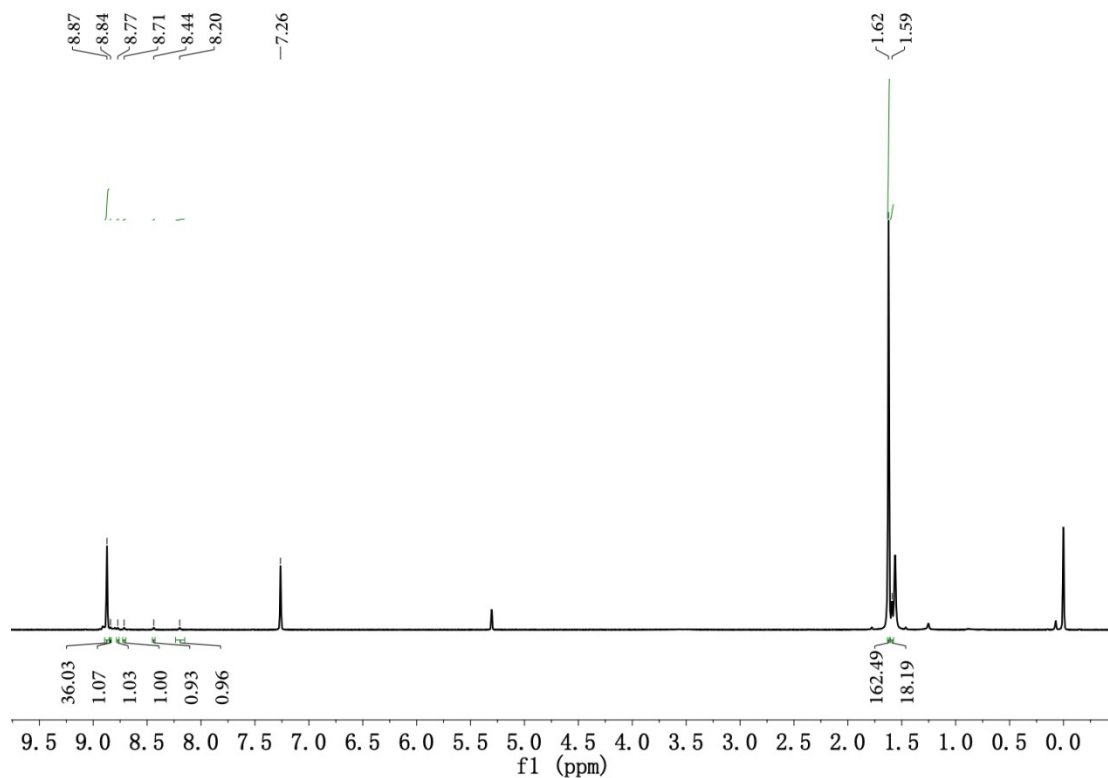


**Figure S1.**  $^1\text{H}$  NMR spectrum of **TriBrPy** and **TetraBrPy** (400 MHz, 293 K,  $\text{CDCl}_3$ ).

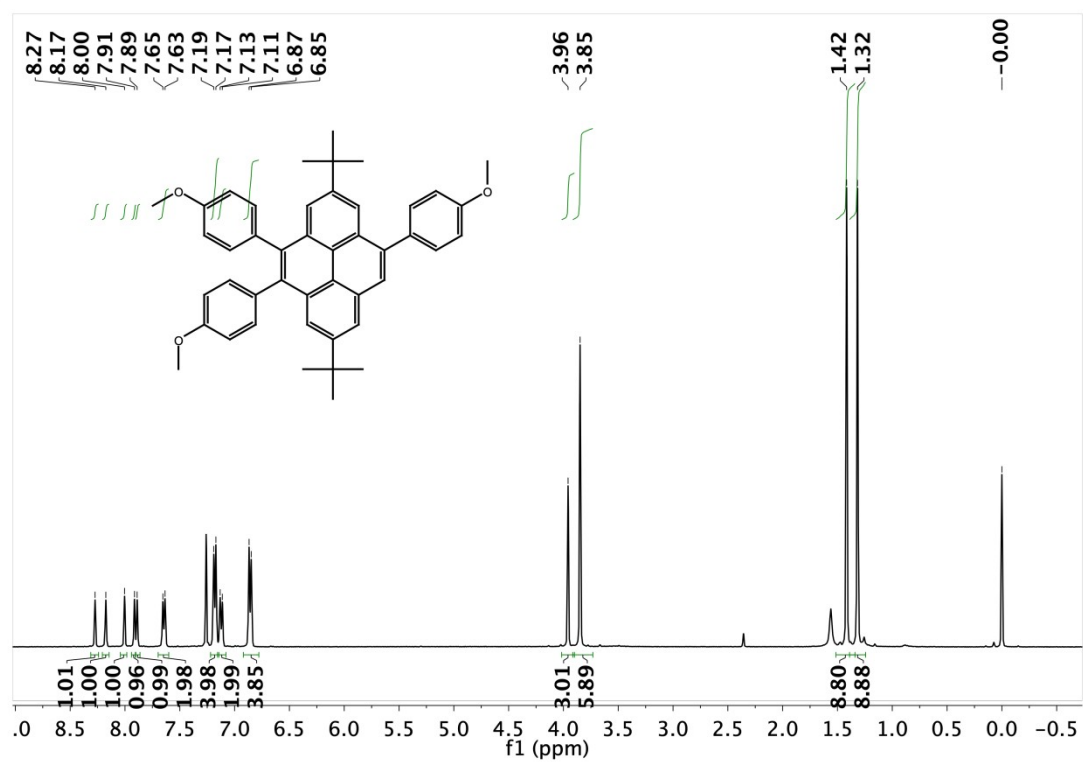


**Figure S2.**  $^1\text{H}$  NMR spectrum of **TriPhPy** (400 MHz, 293 K,  $\text{CDCl}_3$ ).

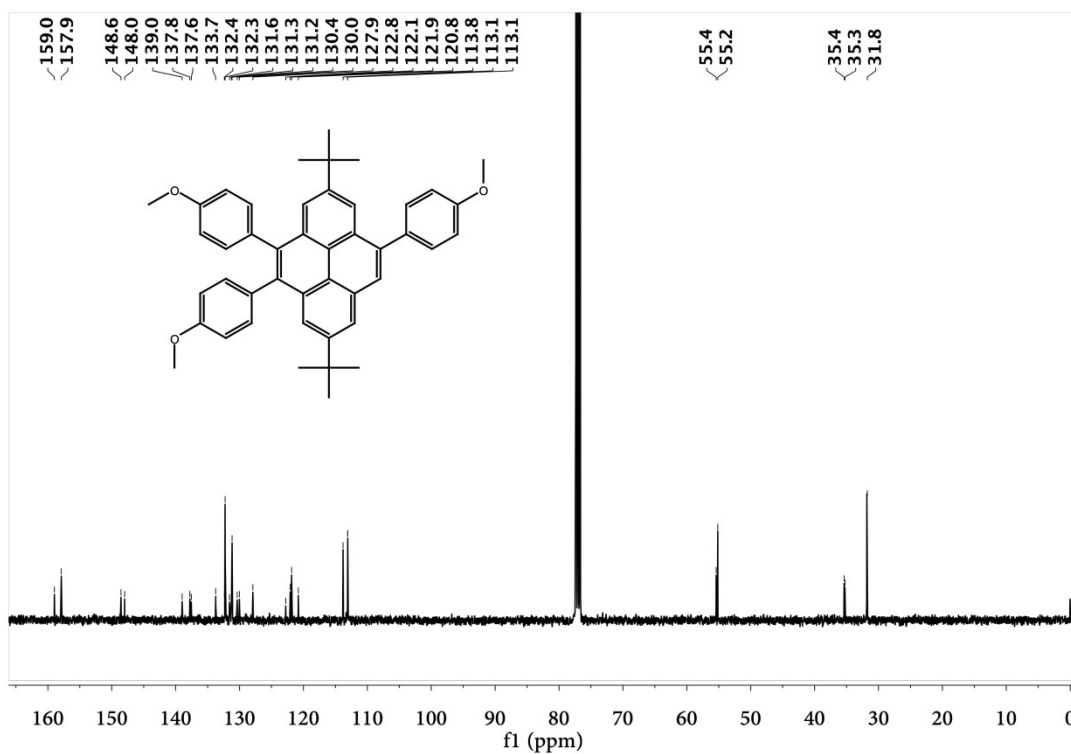


**Figure S3.**  $^{13}\text{C}$  NMR spectrum of **TriPhPy** (100 MHz, 293 K,  $\text{CDCl}_3$ ).

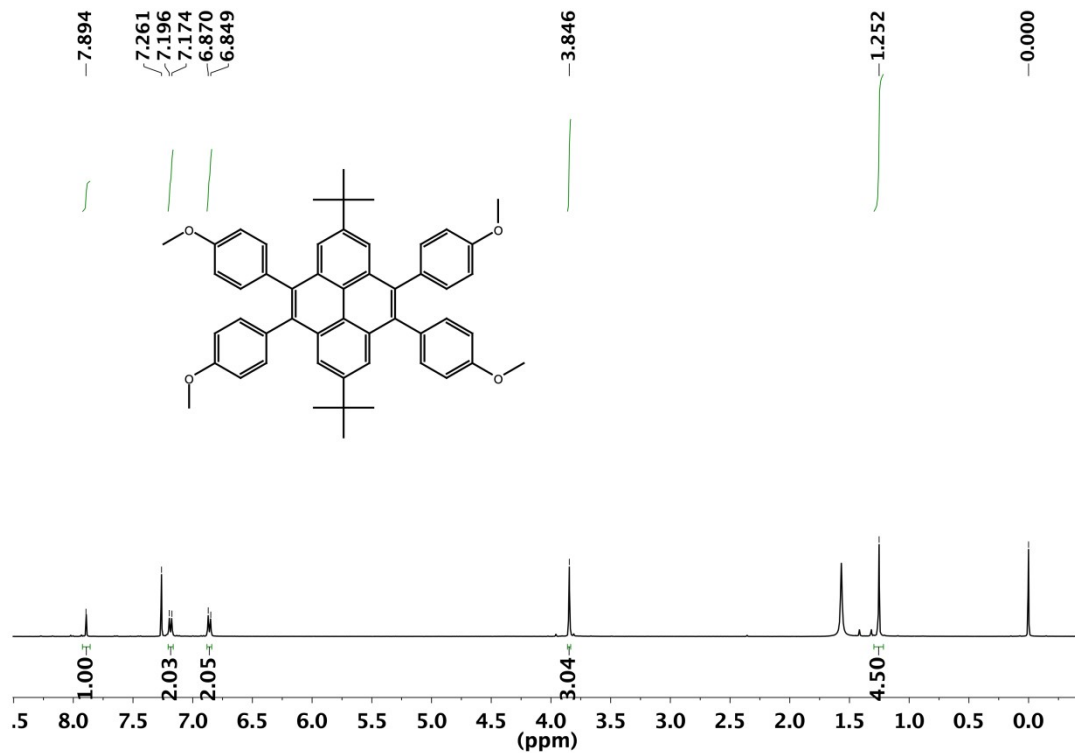


**Figure S4.**  $^1\text{H}$  NMR spectrum of **TetraPhPy** (400 MHz, 293 K,  $\text{CDCl}_3$ ).

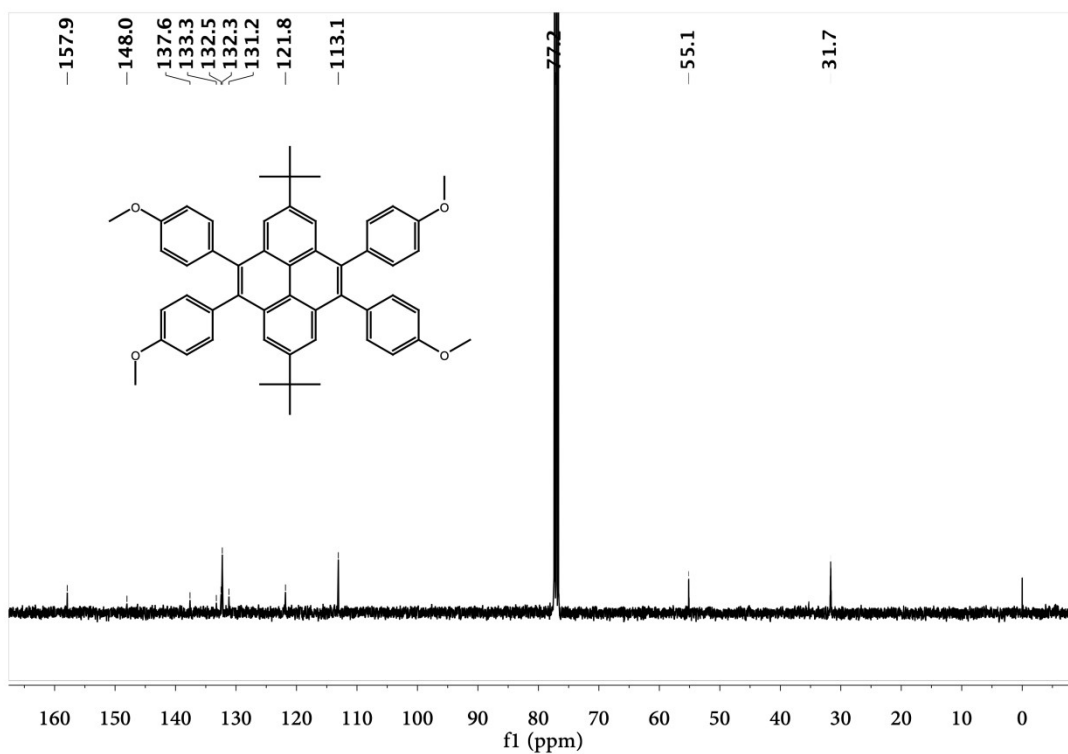


Figure S5.  $^{13}\text{C}$  NMR spectrum of **TetraPhPy** (400 MHz, 293 K,  $\text{CDCl}_3$ ).

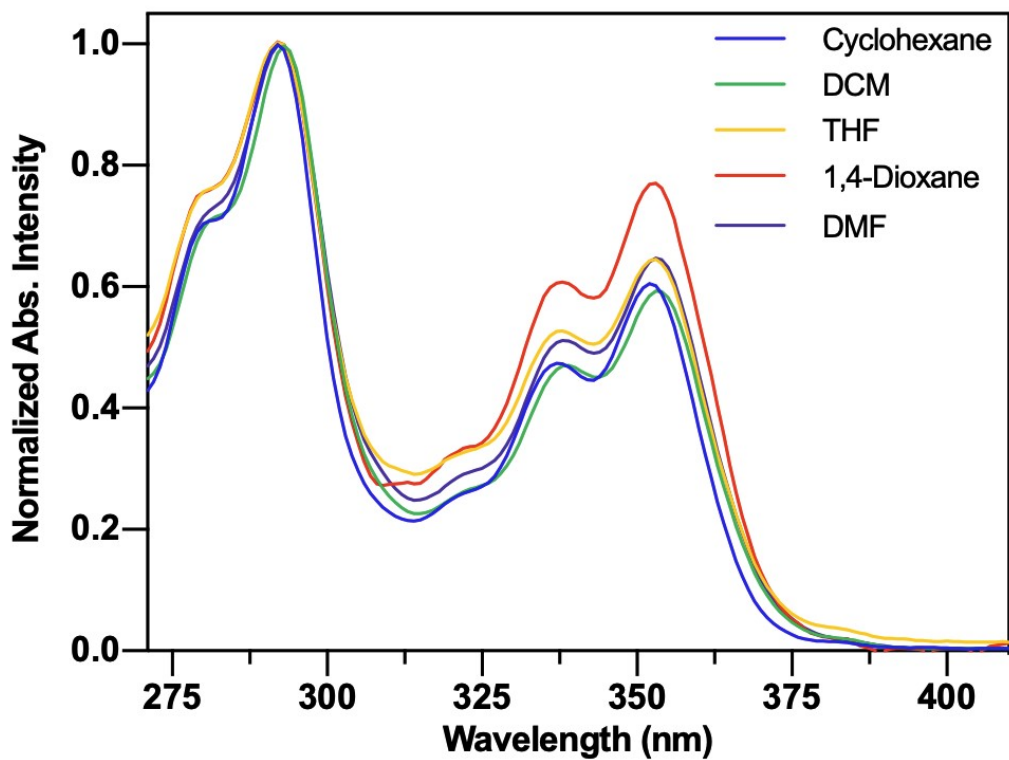
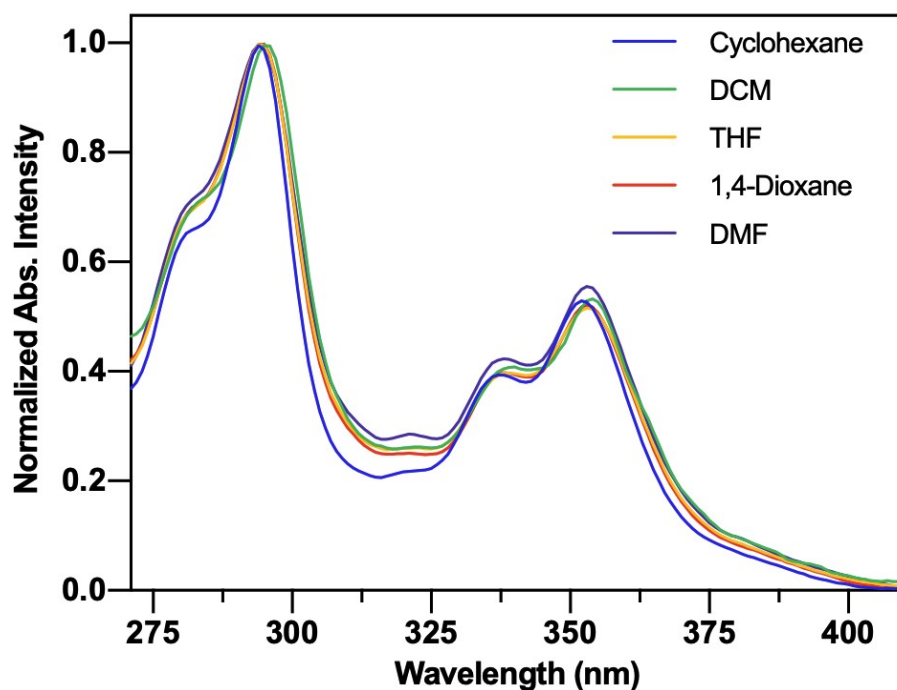
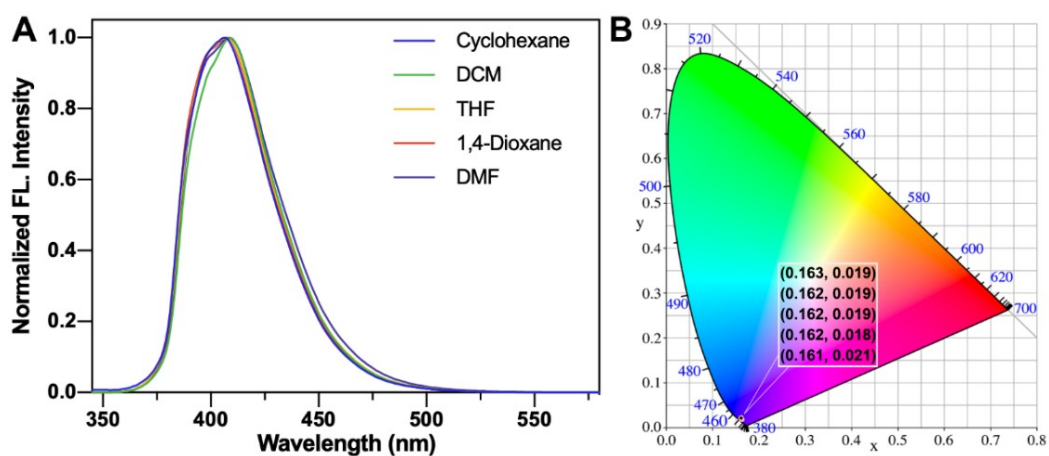


Figure S6. Solvatochromism effect of UV-vis absorbance spectra of **TriPhPy** at a concentration of  $10\ \mu\text{M}$  at  $25\ ^\circ\text{C}$ .



**Figure S7.** Solvatochromism effect of UV-vis absorbance spectra of **TetraPhPy** at a concentration of 10  $\mu\text{M}$  at 25  $^{\circ}\text{C}$ .



**Figure S8.** Solvatochromism effect in the emission spectra (A) and the CIE 1931 chromaticity diagram (B) for **TriPhPy** in cyclohexane, 1,4-dioxane, THF, DCM and DMF, respectively.

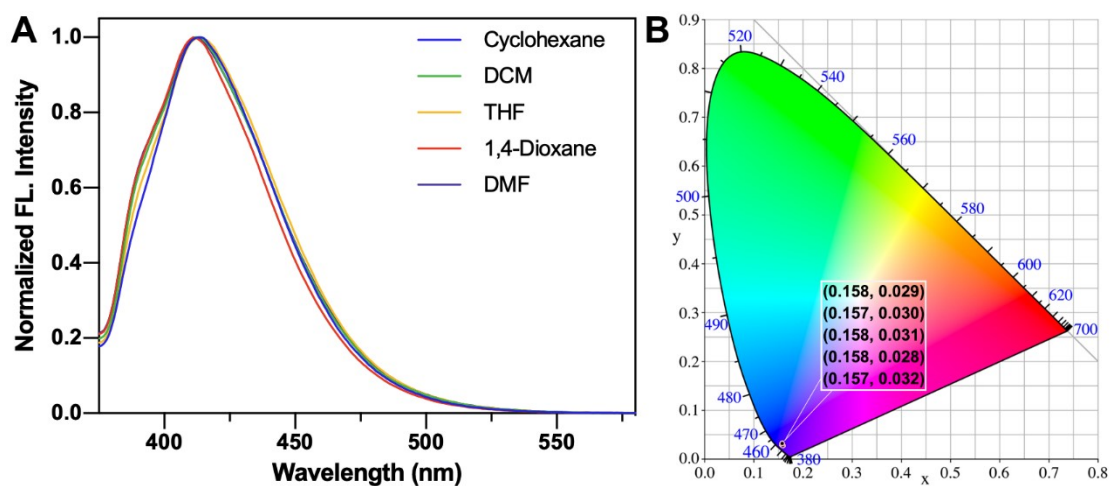


Figure S9. Solvatochromism effect of emission spectra (A) and CIE 1931 chromaticity diagram (B) for **TetraPhPy** in cyclohexane, 1,4-dioxane, THF, DCM and DMF, respectively.

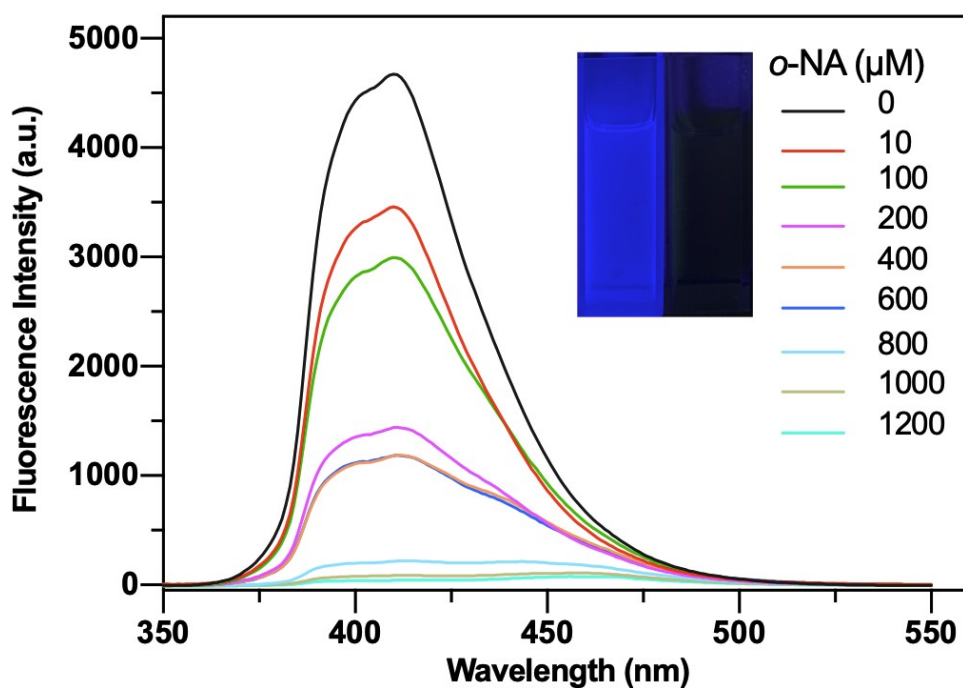


Figure S10. Fluorescence quenching spectra of **TriPhPy** with incremental concentration addition of *o*-NA.

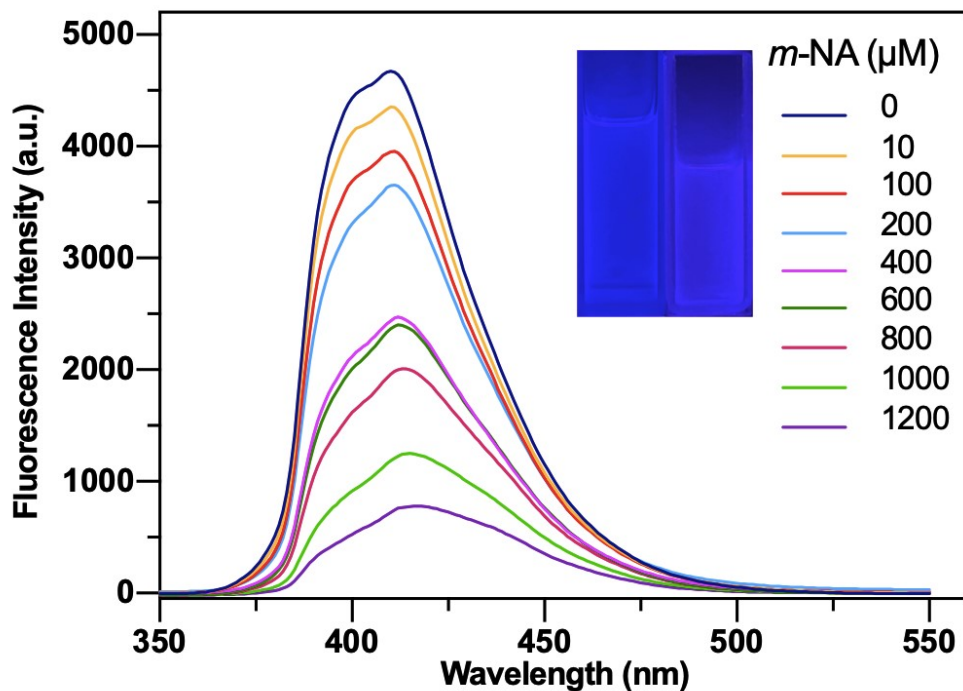


Figure S11. Fluorescence quenching spectra of **TriPhPy** with incremental concentration addition of *m*-NA.

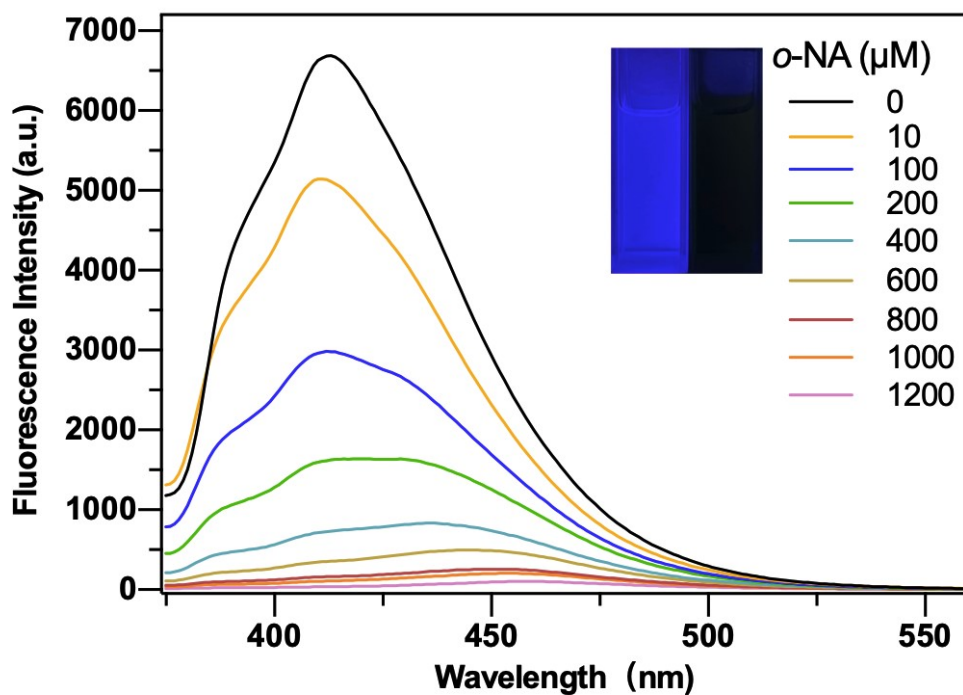
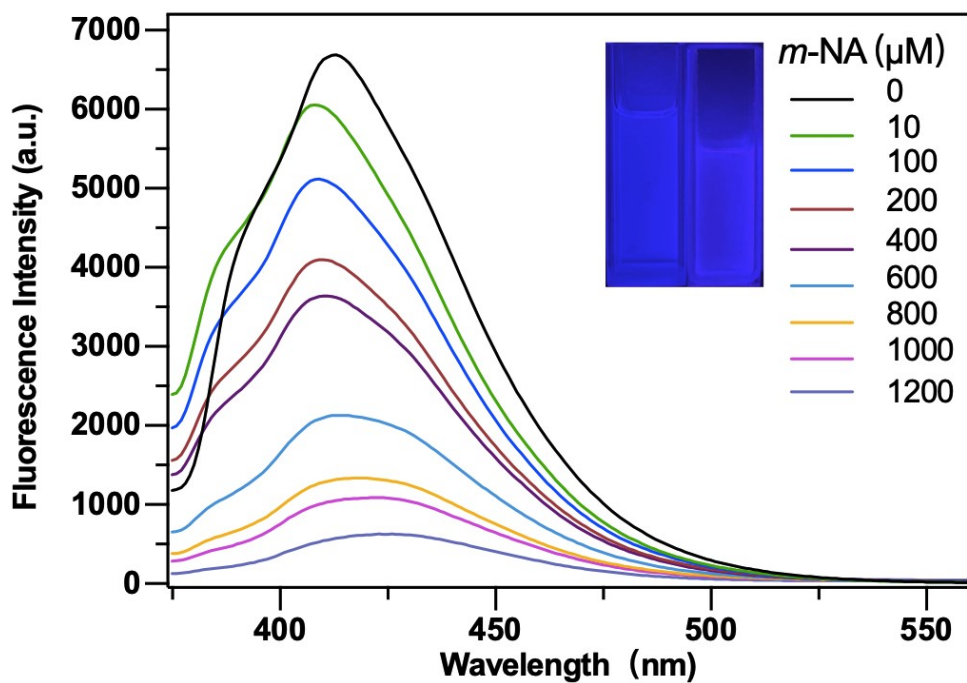
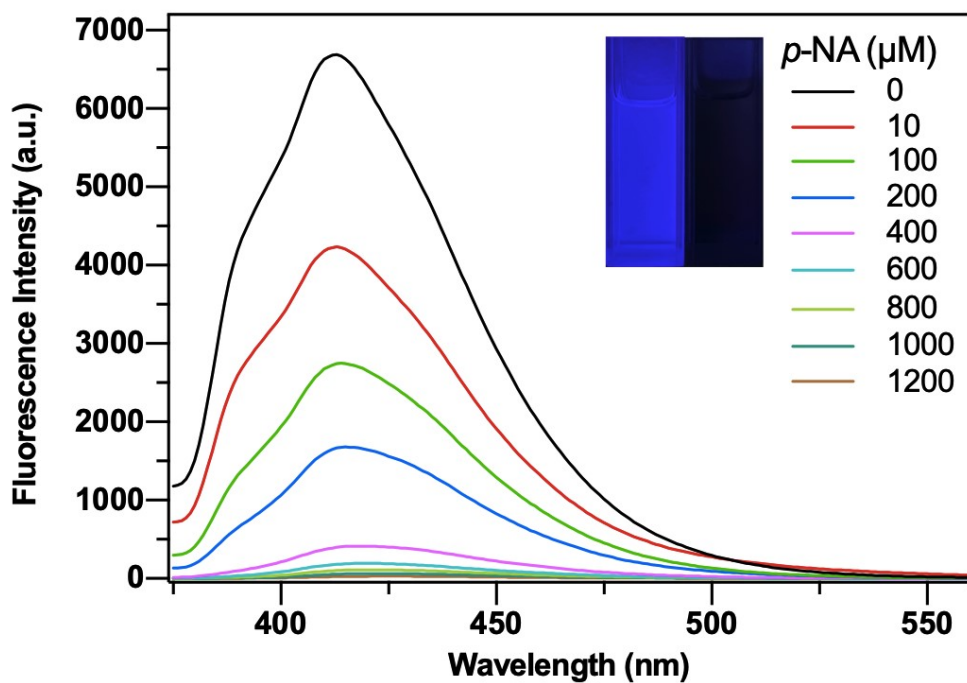


Figure S12. Fluorescence quenching spectra of **TetraPhPy** with incremental concentration addition of *o*-NA.



**Figure S13.** Fluorescence quenching spectra of TetraPhPy with incremental concentration addition of *m*-NA.



**Figure S14.** Fluorescence quenching spectra of TetraPhPy with incremental concentration addition of *p*-NA.



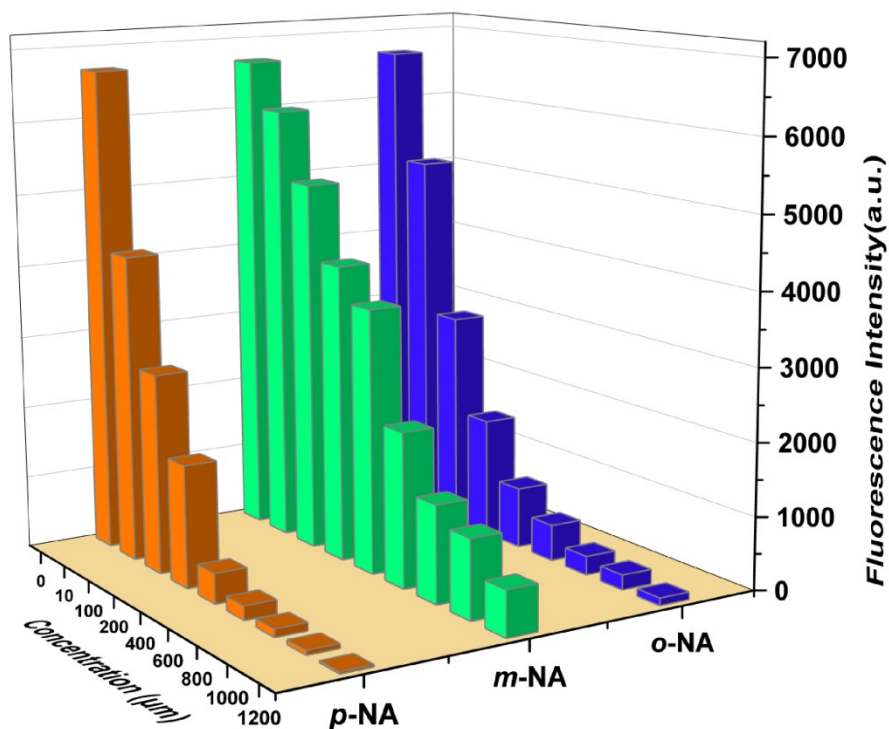


**Figure S15.** Histogram of fluorescence quenching of **TetraPhPy** with NA.

### Standard deviation and detection limit calculations

To calculate the standard deviation and detection limit of this detection method, fine particles of **TriPhPy/TetraPhPy** with fine particles was made into a solution ( $1 \times 10^{-5}$  M, DCM). Then, a nitroaniline (*o*-NA, *p*-NA, *m*-NA) solution (10 mM) was added to the respective solution and the fluorescent intensities were recorded. The standard deviation ( $\sigma$ ) was calculated from five blank tests of **TriPhPy/TetraPhPy** solution (0.0162, 0.1321 respectively) and the limit of detection (LOD) was calculated via the formula:  $3\sigma/K$  ( $K$ : the slope of the linear region). The LODs of **TriPhPy** was calculated to be  $1.25 \times 10^{-8}$  M,  $1.36 \times 10^{-8}$  M for *o*-NA, *m*-NA, the LODs of **TetraPhPy** was calculated to be  $5.62 \times 10^{-8}$  M,  $6.01 \times 10^{-8}$  M,  $6.48 \times 10^{-8}$  M for *o*-NA, *p*-NA, *m*-NA, respectively.